MAGNETIC RESONANCE IN CHEMISTRY, VOL. 35, S29–S36 (1997)

Real Time Investigation of the Freezing of Raw Potato by NMR Microimaging

B. P. Hills,* O. Goncalves, M. Harrison and J. Godward
Institute of Food Research, Norwich Research Park, Colney, Norwich NR4 7UA, UK

Results are presented of an NMR microimaging study of the freezing of raw potato at 253 K. A fast radial imaging technique was used to obtain profiles along the sample radius. The profiles show that there is not a sharply defined ice front moving through the tissue, but rather a region where various fractions of ice and liquid water co-exist whose spatial extent progressively increases. The results are compared with predictions of a generalized Plank model and with numerical solutions of the thermal diffusion equation. Although the integrated profile intensities could be fitted, neither model succeeds in accurately reproducing the image profiles. This suggests that more sophisticated models which take explicit account of the compartmentalized cellular and sub-cellular nature of the tissue may be necessary for understanding the observed imaging data. © **1997 John Wiley & Sons, Ltd.**

Magn. Reson. Chem. **35**, S29–S36 (1997) No. of Figures: 6 No. of Tables: 1 No. of References: 12

Keywords: freezing; potato; magnetic resonance imaging; NMR microimaging

Received 7 February 1997; *revised 3 May 1997*; *accepted 18 May 1997*

INTRODUCTION

Freezing is one of the most common methods of food preservation in use today, and much research has gone into optimizing freezing conditions.[1] Such knowledge is desirable in order to minimize the time and energy requirements, whilst still ensuring that the product is safely frozen. Much of this research involves obtaining experimental data on the freezing of a simple system, and developing mathematical models which can be applied in more complex cases. However, there are still many unresolved questions which require further research. For example, the influence of food composition and microstructure on the amount of non-freezing water and ice at a particular temperature cannot currently be accurately predicted, which makes modelling of specific heats and thermal conductivities an essentially empirical exercise.

Magnetic resonance imaging (MRI) has proved a useful technique in many areas of food research.[2] To observe the processing in small food samples, the microscopic version of the technique is applied. Although MRI microscopy suffers from a lack of resolution as compared with other microscopic techniques, it has the advantage that it is non-invasive. Therefore, images can be obtained whilst various processing operations are in progress without the need to stop and take samples at various intervals. Also, as the same sample is followed throughout the process, problems with maintaining consistency in a number of different trials are avoided.

The basis for the application of MRI to the freezing process is the large drop in the water transverse relaxation time on freezing, and the resultant loss of image intensity. Provided that delays in the pulse sequence are fixed so that essentially all the ice transverse magnetization has decayed whilst a considerable proportion of that of liquid water remains, the ice will be effectively invisible in the image. The microscopic resolution provided by the technique enables the loss of signal at various positions within the sample to be observed. Hence the progress of freezing at different parts of the sample can be distinguished. By comparison of the signal intensity at a given point in space and time with that at the same position at the beginning of the experiment, the ratio of frozen to non-frozen water at that point can be obtained.

The radial imaging technique was first developed in 1991.[3] Although it offers less information than a two-dimensional image, it has a number of benefits. First, as the information can come from a large sized slice, the signal-to-noise (s/n) ratio is good. Second, the information is obtained rapidly. (If a single scan per image is used, which is feasible due to the good s/n ratio, a complete image is obtained in the time for a single echo.) A judicious choice of two-dimensional sequence can offer good s/n ratio or rapid acquisition time, but the combination of both is unique to the radial imaging sequence.

In a previous paper, we presented results on the application of radial imaging to the freezing of rehydrated spaghetti.[4] This process was then modelled by an approximate analytic solution based on a generalized Plank model of freezing as well as by a more exact numerical solution. This system was chosen owing to its cylindrical shape and reasonably homogeneous composition and because radial profile techniques had already been successfully applied to its rehydration[5] and drying.[6] This paper expands this research to cellular tissue by investigating the freezing of raw potato. This presents a number of additional challenges, due

* *Correspondence to*: B. P. Hills.
Contract grant sponsor: Biotechnology and Biological Science Research Council.

 CCC 0749–1581/97/SI0029–08 $17.50

mainly to the fact that different sub-cellular organelles in cellular tissue show very different freezing behaviour,[7] so a sharp ice front moving into the sample during freezing is no longer to be expected. Instead, each temperature is associated with a particular fraction of unfrozen water and ice and it is no longer safe to assume thermal equilibrium. Some (sub)cellular water compartments could remain in an unfrozen, supercooled state, while other (sub)cellular compartments are frozen. This, in turn, could lead to osmotic dehydration of some, but not all, of the cells within the tissue.

In this work we therefore attempted, for the first time, to use microimaging to determine the time course of the unfrozen water profiles (apart from just the position of an ice front). As we shall demonstrate, the hypothesis of an extended domain of unfrozen water is confirmed by the imaging data and this presents a new opportunity to test various theoretical models of freezing. In this exploratory paper we investigate to what extent two very different freezing models succeed in rationalizing the data. The first is the simple Plank freezing model,[8] which has the advantage of providing simple analytical solutions and the disadvantage that it assumes a sharp ice front, which is not observed in the MRI data. The second model is based on numerical solutions to the thermal diffusion equation which does not assume a sharp ice front. As we shall show, neither model provides a very good description of the MRI data and we speculate that it will be necessary to use models which take explicit account of the ice nucleation kinetics, the microstructure of the cellular tissue and the undercooling of selected (sub)cellular water compartments within the tissue.

INSTRUMENTATION AND MATERIALS

MRI set-up

The experiments were conducted on a Bruker MSL-300 spectrometer operating at a proton frequency of 300.13 MHz. It was equipped with a selective pulse excitation unit to generate soft pulses and permit slice selection. Field gradients were supplied by a Bruker microimaging probe fitted with a 20 mm insert. The standard Bruker low-temperature set-up was used. Cooling was achieved via cold, dry nitrogen gas obtained by a slow boil-off of liquid nitrogen. The required temperature was obtained by heating the inflowing gas and monitoring the temperature with a thermocouple. On our Bruker VT unit a heater setting of 8 and a nitrogen boil-off rate of 3 were used.

As part of the preliminary experiments, the behaviour of the Bruker VT unit was investigated. The actual temperature inside the probe was measured by a calibrated thermocouple linked to a micro-logger and the time for the probe to reach equilibrium after a temperature change was measured. The results showed that at least 20 min were required to ensure that the temperature reaches equilibrium inside the probe after a change in the VT thermostat setting.

The one-dimensional radial imaging sequence was identical with that used in the studies of pasta.[4–6] The initial 'hard' 90° excitation pulse had a duration of 23.5 μs and slice selection was achieved via a three-lobed 180° sinc pulse of duration 2.5 ms, applied in the presence of a slice selecting z-gradient of strength 0.60 G cm^{-1} and duration 2.7 ms. A 16.7 G cm^{-1} read-out gradient was applied in the radial direction. The echo time (TE) was 8.7 ms.

The echo obtained from the radial imaging sequence was first Fourier transformed to give a transverse cross-sectional projection and the radial profile was obtained from the projection by an inverse Abel transform. This can be performed using standard mathematical techniques, but a significant improvement in s/n ratio may be achieved using the maximum entropy method.[9] An increase in the s/n ratio of $\sqrt{2}$ can be obtained in either method by taking the average of the right- and left-sides of the projection before transformation.

Potato samples

A large baking potato was used. A long plug of potato was taken from the thickest region using a 9 mm diameter cork borer, and a section a few centimetres in length was cut with a scalpel from the centre of this plug. When taking multiple samples from a single potato, care was taken to ensure that they were obtained from different regions. This was necessary to avoid portions of potato, close to previous sampling points, which had dried out. To minimize moisture loss from newly bored potatoes, they were wrapped in cling-film at all other times.

THE NON-SPATIALLY RESOLVED FREEZING BEHAVIOUR OF POTATO

The non-spatially resolved freezing behaviour was studied by measuring the integrated image intensity in a potato sample as the temperature was progressively lowered in steps. For this experiment a cylindrical potato plug was first sealed in cling-film to prevent moisture loss and placed in the bottom of a sealed 10 mm NMR tube in the microimaging probehead. The probe temperature was then set to 298 K and after a 30 min temperature equilibration time an echo was taken using the radial profile sequence with exactly the same parameter settings as used in the dynamic imaging experiments. The temperature was then decreased to 288 K, a further equilibration time allowed and another echo obtained. This procedure was continued at lower temperatures down to 248 K in 5 K steps. The echoes from the above procedure were Fourier transformed to give the cross-sectional projections, which were integrated to give the total signal as a function of temperature. These data, normalized to the highest signal intensity, are presented in Fig. 1. The results clearly show a freezing transition at around 263 K, which is below the melting temperature (*ca.* 273 K) and suggests that the sample is undercooling at temperatures above 263 K. This is consistent with previous literature observations.[7] The absence of a signal from non-freezing water below the freezing temperature (263 K) is not unexpected, since its transverse relaxation time is

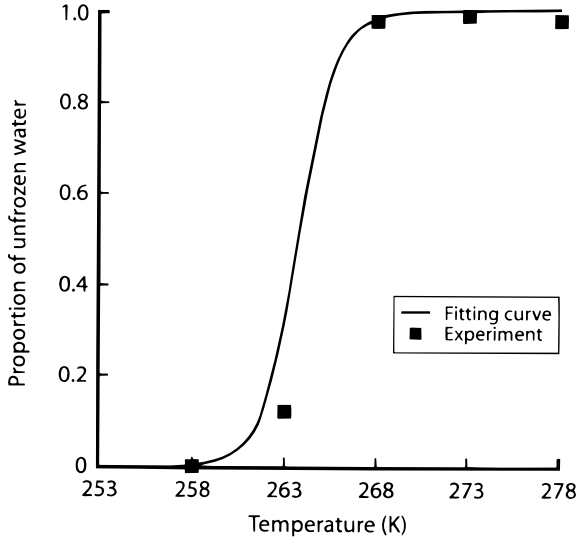

Figure 1. Temperature dependence of the normalized radial profile signal intensity at thermal equilibrium. Note the freezing transition at *ca*. 263 K. The smooth curve is the fit of Eqn (11).

too short to permit its detection via the radial imaging sequence with an echo time of 8.7 ms. The observation that the normalized signal drops from 1 to 0 over a *ca.* 5 K temperature range around 263 K suggests that it is safe to equate the relative image intensity to the fraction of unfrozen water. Previous non-spatially resolved measurements of the temperature dependence of water proton transverse relaxation times in raw potato[7] show that the relaxation time of the unfrozen vacuolar and cytoplasmic fluid is in excess of 100 ms, which is much longer than TE. There should therefore be little distortion of the image profiles by relaxation weighting.

MEASUREMENTS OF POTATO FREEZING IN REAL TIME

Experimental

In order to conduct the real-time freezing experiments, direct contact between the sample and the cooling gas was necessary. This was done to avoid introducing additional thermal barriers to the transfer of heat from the sample surface, which would complicate the modelling process. To achieve this, one end of the potato plug was wrapped in PTFE tape and pressed into the open end of a 10 mm NMR tube. By placing the inverted tube in a standard NMR spinner, the whole assemblage could be easily lowered down the magnet bore into the micro-imaging probehead. Although there was no barrier to avoid water loss, it was assumed that freezing takes place so much faster than drying that water loss could be neglected.

Since the temperature calibrations had shown a 30 min temperature equilibration time, it was decided to introduce the sample into a precooled probe. This would ensure a constant external temperature throughout the experiment, which greatly simplifies the mathematical modelling. Taking account of the previously determined effective freezing point of 263 K, a probe temperature of 253 K was used to ensure effective freezing conditions. As soon as the sample had been placed in the probe, echoes were obtained every 30 s using the radial imaging sequence. This continued until no further signal was obtained, indicating that the sample was completely frozen. No signal averaging was performed, and the echo time was fixed at 2.0 ms. After the data had been obtained, they were Fourier transformed on the spectrometer giving the cross-sectional projections.

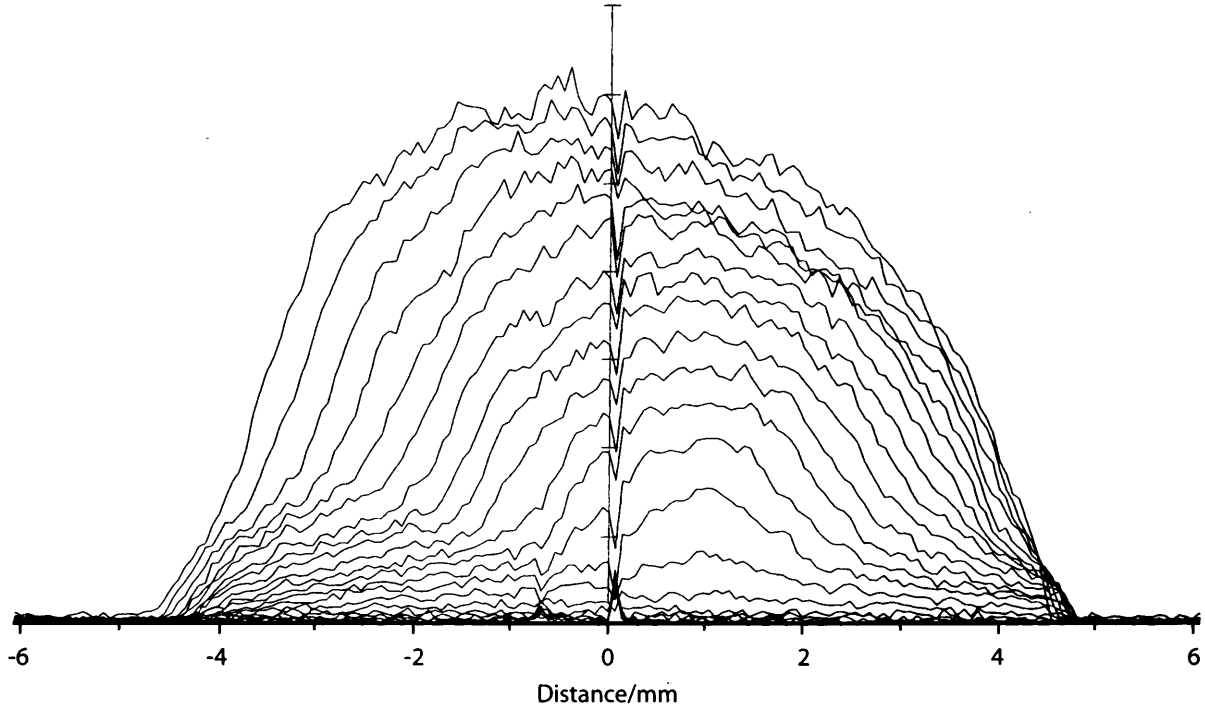

Figure 2. Cross-sectional projections of the freezing of a cylindrical potato sample, initially at room temperature, when placed into a probe at 253 K. Projections were taken at the start of the experiment and 30 s intervals thereafter.

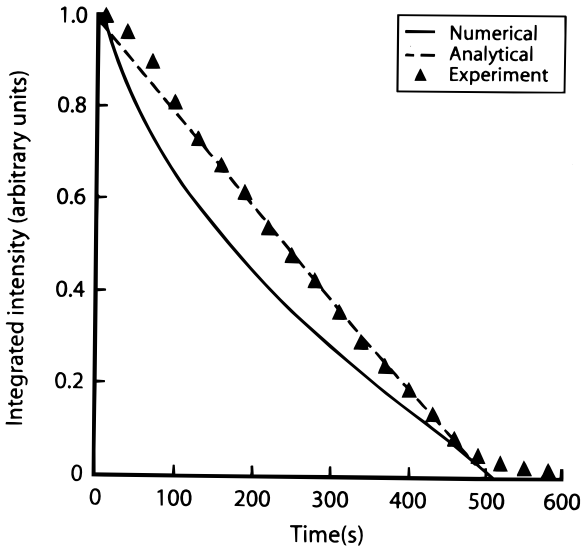

Figure 3. Loss of intensity as a function of time during the freezing of a cylindrical potato sample at 253 K. The dashed line is the fit of the Plank model and the continuous line the fit of the numerical model based on the water parameters in Table 1.

These were then transferred to a PC where inverse Abel transformation was performed by both matrix inversion and maximum entropy methods. Visual observation at both the beginning and end of the experiment confirmed that cylindrical symmetry of the sample, an assumption of the inverse Abel method, was maintained.

Results and discussion

Cross-sectional images from a characteristic freezing run are displayed in Fig. 2. An estimate of 9 min for the freezing time can be made from the first image that shows complete loss of signal. The apparently noisy surface of the images should be noted; at first this was assumed to be due to thermal noise, but an experiment at room temperature, using different amounts of signal averaging, showed that the shape was not smoothed out by increasing the number of scans. This indicates that the behaviour is due to inhomogeneities in the distribution of unfrozen water in the sample itself. The potato cells themselves display some heterogeneity in size and structure and, of course, at the intracellular level the cells differ in the content and size of organelles such as vacuoles, starch granules and cytoplasm, all of which contain different concentrations of water and have slightly different relaxation times.[7] This suggests that there is probably heterogeneity in the size and distribution of ice crystals throughout the tissue. Mention should also be made of the shape of the cross-sections as the freezing progresses. Unlike the case of the freezing of pasta,[4] the profiles do not retain a semi-circular shape as the freezing progresses, but always retain some amount of signal at their edges. This indicates that there is no sharp freezing front within the sample, a fact that will be seen more clearly when the radial profiles themselves are considered.

The cross-sectional projections were integrated to show the loss of signal with time during freezing. These data are displayed in Fig. 3. As it is assumed that ice contributes nothing to the image intensity, this graph may also be used to obtain the fraction of frozen water in the whole sample at any time. The graph is approximately linear, which allows an improved estimate for the time to complete freezing to be obtained. This value is 8 min 45 s.

Figure 4 shows the result of inverse Abel transformation of the cross-sectional projections by matrix inversion with maximum entropy s/n ratio enhancement. The increase in signal close to the sample centre is noteworthy in the final few profiles. This is not a real phenomenon, but is an artifact of the maximum entropy method. The profiles are extremely noisy at these points, which is consistent with the low percentage of liquid water and the small sampling volume in the centre of the almost frozen sample. The effect is caused

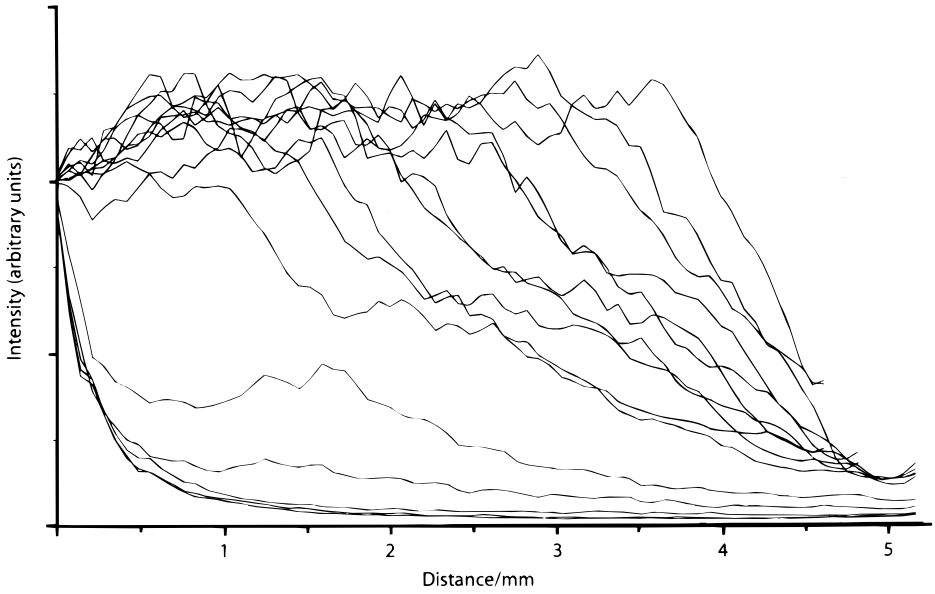

Figure 4. Radial profiles of potato freezing at intervals of 30 s for the first 5 min and 60 s for the next 6 min. The data were obtained by maximum entropy inverse Abel transformation of the projections in Fig. 2.

by the maximum entropy calculation reverting to the initial estimate (called the 'prior') used in the calculation. The data at these particular points must therefore be ignored.

The principle feature of the profiles is the absence of any clearly defined ice front. Instead, there is a range over which ice and liquid water co-exist, with increasing ice content towards the outside of the sample. This behaviour is very different to that of the sharply defined ice front observed in the case of pasta, and is consistent with the previous observation using NMR relaxometry that different sub-cellular compartments such as the cell wall, starch granules and cytoplasm freeze show different freezing behaviour and contain different amounts of unfrozen water at any given sub-zero temperature.[7]

It is also necessary to comment on the meaning of the signal intensity at any individual point. If it is assumed that the sample temperature equilibrates much faster than the ingress of ice and that ice does not contribute to the signal, relating this value to the signal strength of the initial profiles yields the fraction of liquid water at that point.

ANALYTICAL MODELS OF POTATO FREEZING

A generalized Plank model of freezing

There is already a large body of literature concerning freezing time prediction, reflecting the importance of the subject. Most of the models used are approximate analytic solutions based on various modifications of the Plank model,[10] and have been reviewed.[8] In this section, these models are developed for the case of freezing of raw potato, using the results in the previous section as input data. This process resulted in estimates of the surface heat transfer coefficient and thermal conductivity which were then used as first guesses in the numerical model (see later).

The Plank model relies on three assumptions: (i) physical parameters such as thermal conductivity of ice and density of water are constant; (ii) a constant outside temperature; and (iii) a discrete ice–water front. The first condition is assumed to be correct, the second condition was ensured by using a pre-cooled probe, but the third assumption is known to be wrong by observation of the radial profiles themselves. However, as the aim of this simple model is to predict freezing time rather than the method of ice progression, it was decided to continue with the model. The results thus obtained should be treated with caution, but may still prove valuable. As the original analytical solutions of Plank were based on a simple steady-state heat balance in a sample of rectangular shape, it is also necessary to convert to a cylindrical geometry.

The amount of heat liberated at the ice front, Q_{lat}, is given by

$$Q_{lat} = -\lambda \times 2\pi r l \rho (dr/dt) \quad (1)$$

where λ is the latent heat, ρ the density, l the cylinder length and r the radial position of the ice front. Also, the heat lost from the cylinder surface, Q_{surf}, is given by

$$Q_{surf} = h \times 2\pi R l (T_{surf} - T_{out}) \quad (2)$$

where h is the surface heat transfer coefficient, R is the outside radius, T_{surf} the sample surface temperature and T_{out} the outside air temperature. Equating these two values gives the equation for the velocity of the ice front:

$$(dr/dt) = (hR/\lambda\rho r)(T_{out} - T_{surf}) \quad (3)$$

T_{out} is 253 K, the air temperature of the pre-cooled probe. T_{surf} can be eliminated by equating the heat liberated from the surface, Q_{surf}, to that conducted through the ice phase, Q_{ice}, assuming steady-state conditions. Q_{ice} is given by

$$Q_{ice} = k_{ice} \times 2\pi l (T_{surf} - T_{ice})/\ln(r/R) \quad (4)$$

where k_{ice} is the thermal conductivity of ice, assumed constant, and T_{ice} is the freezing temperature. This gives the condition

$$T_{surf} = [hRT_{out} \ln(r/R) - k_{ice} T_{ice}]/[hR \ln(r/R) - k_{ice}] \quad (5)$$

By substituting this expression for T_{surf} and T_{out} into Eqn (3) and integrating, we finally obtain an equation for the time dependence of the position, r, of the ice front;

$$hR\{(r/R)^2 \ln(r/R) + 0.5[1 - (r/R)^2]\}) + k_{ice}[1 - (r/R)^2] = (2hk_{ice}/\lambda\rho R)(T_{ice} - T_{out})t \quad (6)$$

Being a straightforward analytic expression, Eqn (6) is easy to solve numerically for r as a function of time, using standard spreadsheet or mathematical software. The fraction of unfrozen water can then be calculated as $[r(t)/R]^2$.

Results for the Plank model

The analytical expression (6) was solved numerically using the microsoft Excel spreadsheet package. The surface heat transfer coefficient, h, was the only unknown parameter. Its value was varied to find the best fit for the experimental loss of signal intensity with time shown in Fig. 3. In the fitting procedure a further correction of the data was needed because this simple analytical model assumes that an ice front always exists within the sample. Hence it does not take into account the period necessary to cool the surface of the sample to its freezing point. To account for this pre-cooling period, the time origin of the data was adjusted empirically to give the best possible fit with the calculated results. It was found that a pre-cooling period of 20 s gave the best agreement between theory and observation.

As the potato sample consists of about 78% of water,[11] the modelling was carried out using two sets of initial conditions. The first run used values for the latent heat, density and freezing point of water (273 K). This therefore assumes that there is no undercooling. The second used the corresponding values observed for the potato, and assumes undercooling, with a freezing temperature of 263 K (see Fig. 1). This allows an assessment

of the relative merits of the two approaches to be made. Values of all parameters used for the two different runs are presented in Table 1.

The dashed line in Fig. 3 shows the theoretical fit of the Plank model to the data using the water parameters and a value of h of 79.9 W m^{-2} K^{-1}. The corresponding fits using the potato parameters are almost indistinguishable and so are not plotted separately. Simply fitting the Plank model cannot therefore distinguish undercooling and the equilibrium freezing process. However, the value of h needed to fit the data with the potato parameters was slightly higher at 143 W m^{-2} K^{-1}. The Plank model clearly provides a good description of the intensity–time data but, because it assumes a sharp ice–water front, it clearly fails to describe the experimental profiles. In order to describe both the intensity–time data and the profile shapes, it is obviously necessary to use a more sophisticated model based on the thermal diffusion equation. To this we now turn.

A numerical model of potato freezing

The more general theoretical approach builds on the earlier work of Mascheroni and Calvelo,[12] who were interested in calculating the freezing times of meat, and involves numerical solution of the thermal diffusion equation. In cylindrical coordinates the thermal diffusion equation has the form

$$C(w)\rho(w)(\mathrm{d}T/\mathrm{d}t) = (\mathrm{d}/\mathrm{d}r)k(w)(\mathrm{d}T/\mathrm{d}r) + [\mathrm{k}(w)/r](\mathrm{d}T/\mathrm{d}r) \quad (7)$$

where $C(w)$, $\rho(w)$ and $k(w)$ are the apparent specific heat, the density and the thermal conductivity, respectively. These three quantities themselves depend on the ice fraction, $w(r, t)$, at each temperature and radial position in the sample. For the apparent specific heat this functional dependence has the form

$$C(w) = C(0) - wY\,\Delta C_\mathrm{P} - Y[\lambda + \Delta C_\mathrm{P}(T - T_0)](\mathrm{d}w/\mathrm{d}T) \quad (8)$$

where w is the ice fraction at temperature T, $C(0)$ is the specific heat of the unfrozen sample, Y is the water content of the unfrozen sample, ΔC_P is the difference in the specific heats of ice and water, assumed constant, and λ is the latent heat of crystallization of water at T_0. The first two terms give the change in the specific heat of the sample when the water is converted into ice; the last two terms give the latent heat liberated during freezing. The initial value of the unfrozen sample, $C(0)$ was assumed to be constant and equal to the specific heat of raw potato. The thermal conductivity is assumed to depend on the ice fraction according to the linear relationship

$$k(w) = k_\mathrm{pot} + Yw(k_\mathrm{ice} - k_\mathrm{pot}) \quad (9)$$

where k_pot is the thermal conductivity of raw potato and k_ice that of ice, assumed to be independent of temperature over the range of interest. In principle, fitting the experimental profiles can be used to determine $k(w)$. The variation of the density, ρ, on ice fraction is very small compared with the other factors, so this was assumed to be independent of temperature.

In order to quantify the amount of ice and unfrozen water at each temperature in the potato, the sharp freezing transition was modelled with the continuous function

$$w(T) = 1 - 1/\{1 + \exp[-(T - 263.7)]\} \quad (10)$$

This class of continuous function is more general than a discontinuous phase transition at the freezing point (263.7 K), and gives a more stable numerical solution to the heat transfer problem. The fit of Eqn (10) to the experimental freezing data is shown by the smooth line in Fig. 1.

Having defined the various parameters in the model, the time dependence of the temperature and ice-fraction radial profiles was calculated by numerically solving (7) with the following boundary conditions:

$$\begin{array}{lll} t = 0 & T = 273.16\ \mathrm{K} & 0 \leqslant r \leqslant R \\ t > 0 & \mathrm{d}T/\mathrm{d}r = 0 & r = 0 \\ t > 0 & \mathrm{d}T/\mathrm{d}r = -(h/k_\mathrm{gas})[T_\mathrm{surf}(t) - T_\mathrm{out}(t)] & r = R \end{array} \quad (11)$$

where h is the surface heat transfer coefficient and k_gas is the thermal conductivity of the cooling nitrogen gas in the stagnant gas layer at the sample surface. T_out is the temperature of the cooling nitrogen gas (253 K). The time dependence of the surface temperature, $T_\mathrm{surf}(t)$, was used to modify the boundary condition in Eqn (12) at each iteration of the calculation. The parameter values used in the numerical simulation are included in the Water column of Table 1.

The resulting profiles of temperature and unfrozen water are shown in Figs 5 and 6 and the time evolution of the integrated intensity is shown by the continuous line in Fig. 3. It can be seen that, despite its increased complexity, the numerical model still does not succeed in fitting the freezing data any better than the simple Plank model. The integrated intensities in Fig. 3 are

Table 1. Values of parameters used for the analytical modelling process

Parameter	Water	Potato
Latent heat, λ (J kg^{-1})	3.36×10^5	2.58×10^5
Density, ρ (kg m^{-3})	1000	1100
Potato radius, R (mm)	4.5	4.5
Thermal conductivity of ice, k_ice (Wm^{-1} K^{-1})	2.3	2.3
Ice freezing temperature, T_ice (K)	273	263
Specific heat difference, ΔC_P (J K^{-1} kg^{-1})	—	2130
Specific heat, $C(0)$ (J K^{-1} kg^{-1})	—	3430
Outside air temperature, T_out (K)	253	253
Heat transfer coefficient, h (Wm^{-2} K^{-1})	79.9	143

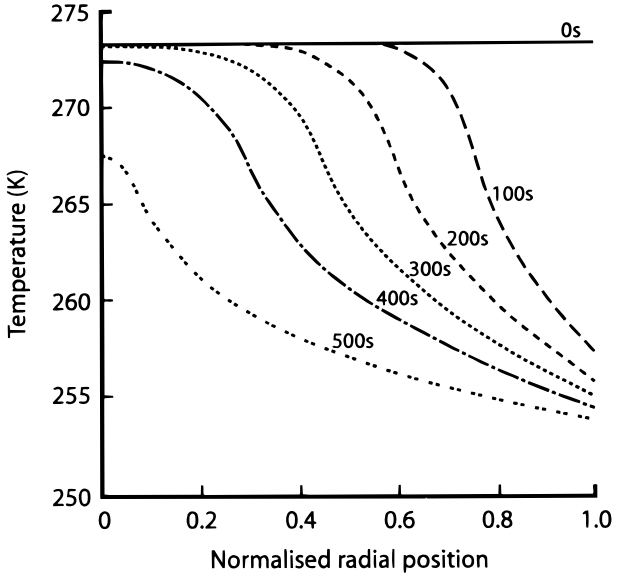

Figure 5. Temperature profiles calculated using the numerical model (see text) for the indicated times and using the parameters in the water column of Table 1.

actually a slightly worse fit. Moreover, the model still predicts an ice front moving into the sample, although it is slightly more sigmoidal in shape than the step function predicted by the Plank model. In neither case is the change of slope observed in the radial image profiles correctly predicted. This suggests that the simple expressions used for the specific heats and thermal conductivities in the numerical model may not accurately reflect the complex nature of the progressive freezing of the various water compartments in the potato tissue and a more sophisticated model which explicitly considers the (sub-)cellular structure of the tissue, the nucleation kinetics and rate of ice crystal growth may be required.

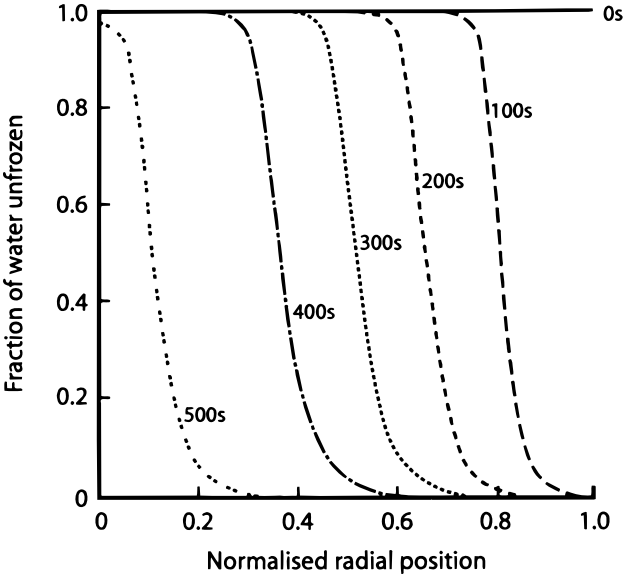

Figure 6. Unfrozen water profiles calculated using the numerical model (see text) for the indicated times and using the parameters in the water column of Table 1.

DISCUSSION

The radial imaging sequence was successfully applied in a quantitative study of freezing in a sample of raw potato. Although there have been previous qualitative MRI studies on the ingress of the ice front into peach halves,[13] this is the first attempt to use MRI to investigate the distribution of unfrozen water and ice in cellular tissue at such a time-scale and resolution. The results clearly show that the ice does not move as a sharply defined front, but rather that there is a spatial region over which ice and liquid water co-exist, with increasing ice content towards the outside of the sample. These observations are believed to be due to the complex microstructure of the potato, which consists of many different subcellular compartments displaying different freezing behaviour.[7]

It is surprising that the Plank model can be made to fit the intensity data so well despite the absence of a sharp ice front which is a central assumption in the model. It is also salutory that the numerical model based on the finite difference solution of the thermal diffusion equation gives an inferior fit to the intensity data and still does not succeed in reproducing the changing slope in the radial profiles of unfrozen water.

The MRI results show that it will be necessary to use a more sophisticated freezing model which explicitly recognizes the cellular structure of the tissue as well as the nucleation and ice-crystal growth kinetics, and this will be the subject of further modelling work. There is also the possibility that some form of 'channelling' of the ice front through the sample is occurring, perhaps along vascular structures in the tissue, in which case some form of fractal freezing model may be required.

Acknowledgements

The authors gratefully acknowledge the financial support of the Biotechnology and Biological Sciences Research Council. They are grateful to Professor G. J. Martin for permitting O. Goncalves to undertake this research as part of a DEA ERASMUS exchange programme with the University of Nantes, France.

REFERENCES

1. W. B. Bald (Ed.), *Food Freezing: Today and Tomorrow*. Springer, Berlin (1991).
2. M. J. McCarthy, *Magnetic Resonance Imaging in Foods*. Chapman & Hall, New York (1994).
3. P. D. Majors and A. Caprihan, *J. Magn. Reson.* **94**, 225 (1991).
4. B. P. Hills, J. Godward, K. M. Wright and M. Harrison, *Appl. Magn. Reson.* **12**, 529 (1997).
5. B. P. Hills, F. Babonneau, V. M. Quantin, F. Gaudet and P. S. Belton, *J. Food Eng.* **27**, 71 (1996).
6. B. P. Hills, J. Godward and K. M. Wright, *J. Food Eng.* (in press).

7. B. P. Hills and G. LeFloch, *Food Chem*. **51**, 331 (1994).
8. H. S. Ramaswamy and M. A. Tung, *J. Food Process Eng*. **7**, 169 (1984).
9. B. Buck and V. A. Macaulay (Eds), *Maximum Entropy in Action*. Clarendon Press, Oxford (1991).
10. A. C. Cleland and R. L. Earle, *J. Food Sci*. **44**, 958 (1979).
11. S. L. Polley, O. P. Snyder and P. Kotnour, *Food Technol*. Nov., 76 (1980).
12. Mascheroni and Calvelo, *J. Food Sci*. **47**, 1201 (1982).
13. M. J. McCarthy and R. J. Kauten, *Trends Food Sci. Technol*. **1**, 134 (1990).

